Research Article

For reprint orders, please contact: reprints@futuremedicine.com

Nanomedicine

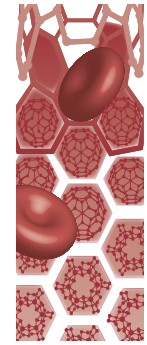

# Uptake of ferromagnetic carbon-encapsulated metal nanoparticles in endothelial cells: influence of shear stress and endothelial activation

**Aim:** Magnetic field guided drug targeting holds promise for more effective cancer treatment. Intravascular application of magnetic nanoparticles, however, bears the risk of potentially important, yet poorly understood side effects, such as off-target accumulation in endothelial cells. **Materials & methods:** Here, we investigated the influence of shear stress (0–3.22 dyn/cm$^2$), exposure time (5–30 min) and endothelial activation on the uptake of ferromagnetic carbon-encapsulated iron carbide nanomagnets into endothelial cells in an *in vitro* flow cell model. **Results:** We found that even moderate shear stresses typically encountered in the venous system strongly reduce particle uptake compared with static conditions. Interestingly, a pronounced particle uptake was observed in inflamed endothelial cells. **Conclusion:** This study highlights the importance of relevant exposure scenarios accounting for physiological conditions when studying particle–cell interactions as, for example, shear stress and endothelial activation are major determinants of particle uptake. Such considerations are of particular importance with regard to successful translation of *in vitro* findings into (pre-)clinical end points.

**Keywords:** cellular uptake • flow model • inflammation • magnetic nanoparticles

Melanie Jacobson[1,2], Birgit Roth Z'graggen[1,2], Sereina M Graber[3], Christoph M Schumacher[4], Wendelin J Stark[4], Claudia Dumrese[5], Jose Maria Mateos[5], Caroline Aemisegger[5], Urs Ziegler[5], Martin Urner[1,2], Inge K Herrmann[‡,1,2,6] & Beatrice Beck-Schimmer[*,‡,1,2]

[1]Institute of Anesthesiology, University Hospital Zurich, Hof E 111, Rämistrasse 100, CH-8091 Zurich, Switzerland
[2]Institute of Physiology & Zurich Center for Integrative Human Physiology, University of Zurich, Winterthurerstrasse 190, CH-8057 Zurich, Switzerland
[3]Anthropological Institute & Museum, University of Zurich, Winterthurerstrasse 190, CH-8057 Zurich, Switzerland
[4]ETH Zurich, Institute for Chemical & Bioengineering, Vladimir-Prelog-Weg 1, CH-8093 Zurich, Switzerland
[5]Center for Microscopy & Image Analysis, Winterthurerstrasse 190, CH-8057 Zurich, Switzerland
[6]Department Materials Meet Life, Swiss Federal Laboratories for Materials Science & Technology (Empa), Lerchenfeldstrasse 5, 9014 St Gallen, Switzerland
*Author for correspondence:
Tel.: +41 44 255 56 32
Fax: +41 44 255 44 09
beatrice.beckschimmer@uzh.ch
‡Authors contributed equally

Diagnostic and therapeutic strategies based on magnetic nanoparticles show great promise and may significantly influence cancer therapy by enabling novel treatment modalities such as targeted drug delivery or early detection of circulating tumor cells [1,2]. Drug delivery through the use of magnetic nanoparticles presents several advantages over the conventional intravenous administration of drug molecules or particles [3,4]. The magnetization of the particle core enables stirring of nanocarriers to the desired location in the body by applying magnetic gradient fields, thereby partially superimposing natural biodistribution. Additionally, surface functionalization allows specific tailoring of the nanocarrier for the required application, hence further minimizing unwanted side effects [5]. While superparamagnetic iron oxide nanoparticles (SPIONs) show colloidal stability and biocompatibility and have successfully been used as contrast agents, such particles suffer from comparatively low magnetization and hence limited targeting efficiency [6]. Recently, ferromagnetic carbon-encapsulated iron carbide nanoparticles with much higher saturation magnetization (>three-times higher compared with conventional magnetic iron oxide nanoparticles) have been synthesized and show promise in overcoming major limitations of weakly magnetic iron oxide nanoparticles [6–10].

Opportunities of magnetic nanoparticles are numerous, but so are potential risks of magnetic drug delivery. Magnetic targeting seems to be feasible in theory, however, encounters significant limitations when translated into *in vivo* systems [11]. Among these limitations, unwanted interactions with non-target cells and tissue is the most critical one, both affecting targeting efficiency and safety of the treatment. Apart from uptake into organs with high phagocytic activity, such as the liver and spleen, interactions with

Future Medicine part of fsg

the endothelial lining of the vessel wall are likely to occur following intravascular application of nanoparticles. Vascular endothelium sites are exposed to considerably varying dynamic blood flow-induced forces, potentially influencing particle uptake under *in vivo* conditions [12]. The shear stresses spectrum in the venous compartment ranges from 0.5 (small veins) to 6 dyn/cm$^2$. In arteries, shear stresses are typically in the order of 5–10 dyn/cm$^2$ for nonaortic vessels, and >15 dyn/cm$^2$ in the aorta. While studies on biodistribution require *in vivo* testing (because of the system complexity that cannot be adequately addressed by *in vitro* models), the interactions of nanoparticles with the vessel wall can be examined under physiologically relevant, well-standardized *in vitro* conditions. These models benefit from the fact that parameters, such as shear stress and flow geometry, can be accurately controlled and monitored as opposed to the typically much more complex *in vivo* situation encountered, hence allowing direct comparison of a variety of different exposure conditions.

Here, we investigated the influence of shear stress, exposure time and endothelial activation on particle uptake in a standardized flow chamber, representing an *in vitro* model of the vascular compartment. In order to mimic blood circulation, we used a dynamic model based on a medium-perfused flow chamber lined with human aortic endothelial cells (HAECs). Shear stresses comparable to those encountered in human venous blood vessels, representing the compartment in contact with the nanoparticles after intravenous injection, were applied to investigate the uptake of carbon-coated iron-carbide nanoparticles. We investigated endothelial uptake of magnetic nanoparticles comparing high (3.22 dyn/cm$^2$) and low (0.57 dyn/cm$^2$) shear stress of the venous system, and static conditions at two time points (5 and 30 min) in unstimulated and human TNF-α-activated cells. This study provides insights into accumulation of particles in the endothelial lining and helps to identify physiologically relevant factors, such as shear stress, inflammation and exposure time governing particle uptake also in *in vivo* settings.

## Materials & methods

### Cell culture conditions

Human aortic endothelial cells (HAECs; Lonza group Ltd, Visp, Switzerland) were cultured in Clonetics™ EGM™-2 BulletKit™ medium (CC-3162)/10% fetal bovine serum (FBS, Life Technologies, Zug, Switzerland) at 37°C, 5% $CO_2$ in a humidified surrounding.

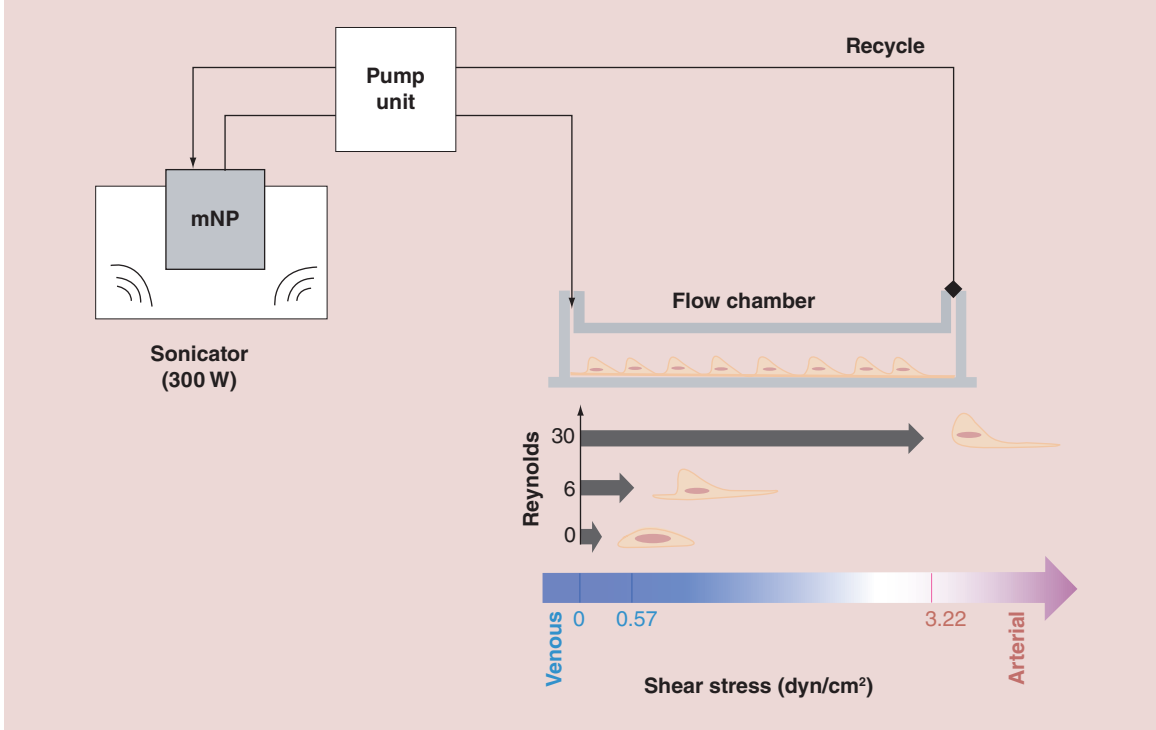


**Figure 1. Experimental setting.** Closed loop system with endothelial cell-lined flow chamber. Magnetic nanoparticles were continuously sonicated throughout the duration of the experiment using a sonicator. They were then pumped through a closed-loop circuit through an endothelial cell-lined flow chamber. The influence of shear stress (0–3.22 dyn/cm$^2$), exposure time and endothelial cell activation on magnetic nanoparticle uptake was studied under standardized conditions.
mNP: Magnetic nanoparticle.

The culture medium was changed every second day. When reaching 80% confluency cells were passaged for experimental approaches, detaching them with 0.05% trypsin (Life Technologies, Zug, Switzerland) and seeding them into the according plates, pre-coated with fibronectin (Millipore, Zug, Switzerland). Only passages 5–9 were used for experiments.

## Nanomagnets

Iron-carbide nanomagnets ($C/Fe_3C$) with a primary particle diameter of 30 nm and a magnetic saturation magnetization of 123 emu/g, functionalized with PEG chains of a molecular weight of 10 kDa, were provided by the Institute for Chemical and Bioengineering, ETH Zurich. They were synthesized as described by Herrmann *et al.* [8]. For each experiment, a nanoparticle dispersion of 10 mg/ml in double distilled water was prepared and sonicated for 10 min in a glass tube on ice, diluted in EBM-2 medium (Lonza, Visp, Switzerland) with 1% FBS to obtain the final concentration. Additionally, nanomagnets were continuously sonicated for the entire dynamic experiments in order to ensure dispersion of the particles.

## Experimental protocols

### Flow model

A total of $6 \times 10^5$ cells/ml in 250 µl culture medium were transferred to a fibronectin precoated µ-slide I $^{0.6}$ Luer (ibidi Treat Chamber 80176; ibidi GmbH, Planegg/Martinsried, Germany). After 2 days cells reached 90% confluency and were incubated with 0.1 mg/ml magnetic nanoparticles in EBM-2/1% FBS medium using 0, 0.57 and 3.22 dyn/cm$^2$ shear stress with exposure periods of 5 or 30 min at 37°C. The same experiments were performed with recombinant human TNF-α 1 ng/ml (BD Pharmingen, Basel, Switzerland), pre-incubating the cells with TNF-α for 4 h before exposing them to nanoparticles. As negative control for TNF-α prestimulation, slides were incubated with EBM medium/1% FBS only.

Shear stress depends on flow rate and the chamber slide geometry, which simulates the vessel diameter and the wall characteristics. Considering medium viscosity containing 0.1 mg/ml magnetic particles identical to that of water, we used the chamber slide manufacturer's formula to calculate shear stress to apply during the experiments with the pump. The following formula was used: shear stress = flow rate pump × 0.603.

A closed perfusion system was designed, consisting of a pump (ISMATEC, Wertheim, Germany), 3-stop silicon peroxide tubes (SCO113 ISMATEC) and a chamber (µ-slide I $^{0.6}$ Luer) with a monolayer of HAECs (Figure 1). Before exposing the cells to the flow the installation was calibrated and rinsed with 70% ethanol, followed by EBM/1% FBS medium until bubbles disappeared. Due to the continuous sonication of the magnetic nanoparticles in medium, the pH of the medium was maintained at 7.0 with Hepes 1 M (Life Technologies). A total of 35 ml of medium EBM2/1% FBS at 37°C containing 0.1 mg/ml of nanoparticles was used for continuous perfusion of the chamber with the cell culture applying low (0.57 dyn/cm$^2$) or high (3.22 dyn/cm$^2$) flow rates according to manufacturer data for the µ-slide I $^{0.6}$ Luer. Cells were kept at 37°C on a heating plate, the medium in a controlled 37°C ultrasonic water bath. As negative control, slides were incubated with EBM medium 1% FBS only without particles for the shear stresses and perfusion times as mentioned above. The same experiments were performed with cells, prestimulated with recombinant TNF-α.

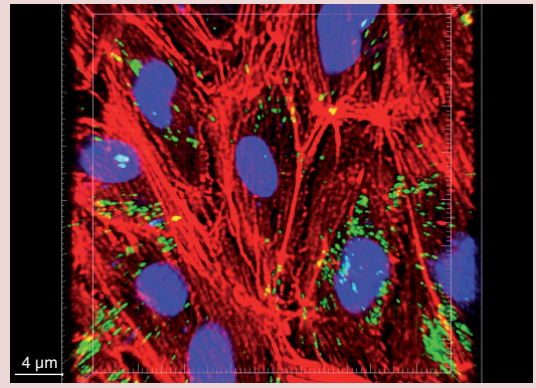


**Figure 2. Intact endothelial cells containing intracellular carbon-encapsulated iron carbide nanomagnets.** A maximum intensity projection of a confocal 3D dataset of human aortic endothelial cells, 4 h prestimulated with TNF-α, followed by an incubation of 30 min with 0.1 mg/ml magnetic nanoparticle under high shear stress. Actin staining in cytoplasma with phalloïdine Alexa 568 (red), nucleus with 4′6′ diamindine-2′phenylindole dihydrochloride (blue) and magnetic nanoparticle (green) visualized using a 488-nm wavelength argon laser in the reflection mode.
Size bar (left lower corner): 4 µm.

## Static inflammation model

A total of $6.5 \times 10^4$ HAEC/ml were cultured in fibronectin-precoated 48-well multiwell plates (BD Falcon™, San Jose, USA) in 250 µl culture medium until they reached 90% confluency. The culture medium was replaced by EBM/1% FBS 250 µl per well 24 h before the experiments were started. Human aortic endothelial cells were stimulated with 1 ng/ml TNF-α for 4 h (control EBM/1% FBS only), followed by an incubation with 0.1 mg/ml magnetic nanoparticles for 2 and 4 h.

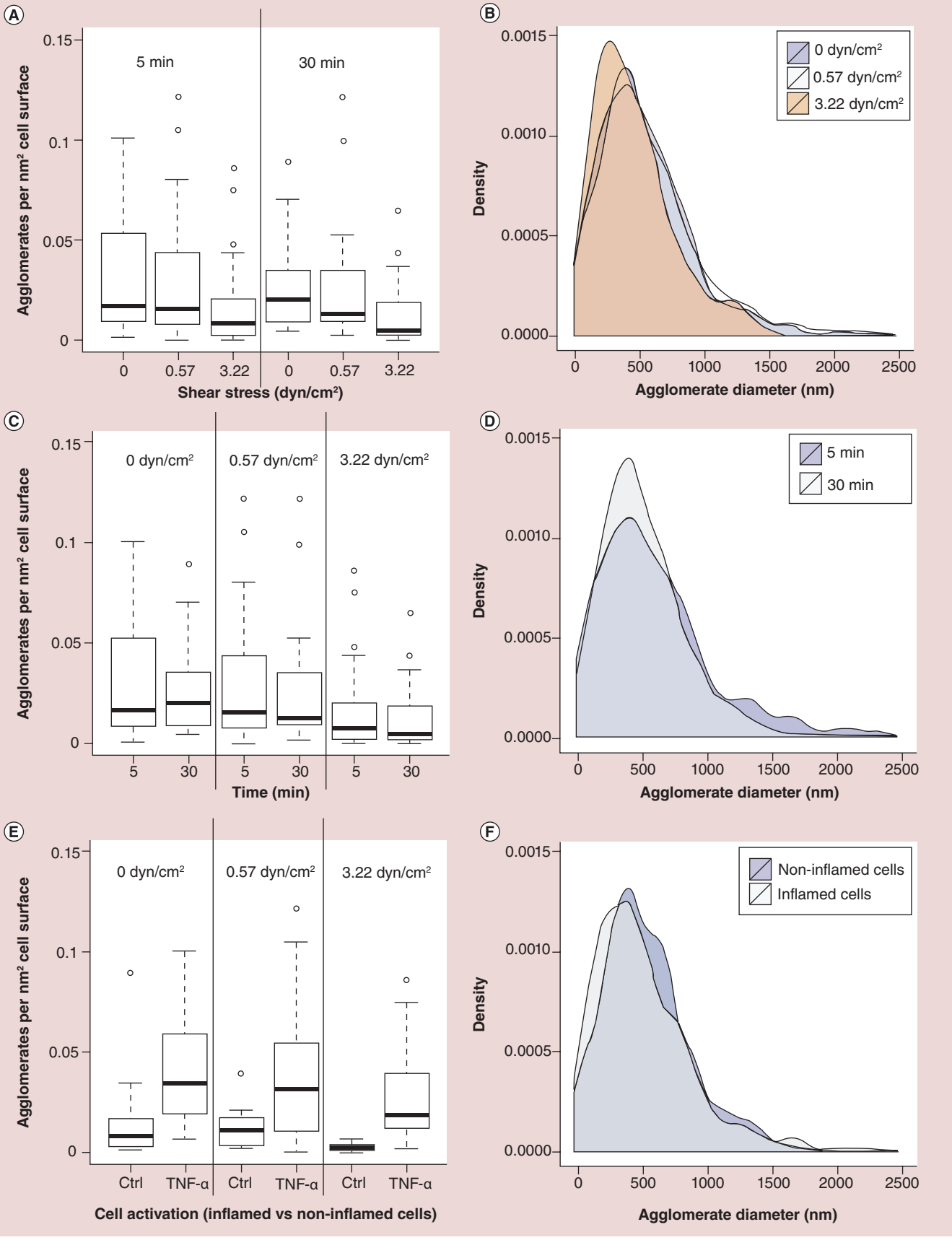
A
Agglomerates per nm² cell surface
0.15
0.1
0.05
0
5 min
30 min
0
0.57
3.22
0
0.57
3.22
Shear stress (dyn/cm²)
B
Density
0.0015
0.0010
0.0005
0.0000
0 dyn/cm²
0.57 dyn/cm²
3.22 dyn/cm²
0
500
1000
1500
2000
2500
Agglomerate diameter (nm)
C
Agglomerates per nm² cell surface
0 dyn/cm²
0.57 dyn/cm²
3.22 dyn/cm²
5
30
5
30
5
30
Time (min)
D
Density
5 min
30 min
Agglomerate diameter (nm)
E
Agglomerates per nm² cell surface
0 dyn/cm²
0.57 dyn/cm²
3.22 dyn/cm²
Ctrl
TNF-α
Ctrl
TNF-α
Ctrl
TNF-α
Cell activation (inflamed vs non-inflamed cells)
F
Density
Non-inflamed cells
Inflamed cells
Agglomerate diameter (nm)

**Figure 3. Magnetic nanoparticle uptake in endothelial cells (see facing page).** Influence of shear stress 0, 0.57 and 3.22 dyn/cm$^2$ on uptake: **(A)** number of intracellular agglomerates of nanoparticles; **(B)** mean diameter of intracellular agglomerates of nanoparticles. Influence of time on uptake: **(C)** number of intracellular agglomerates of nanoparticles; **(D)** mean diameter of intracellular agglomerates of nanoparticles. Influence of prestimulation of endothelial cells on uptake: **(E)** number of intracellular agglomerates of nanoparticles; **(F)** mean diameter of intracellular agglomerates of nanoparticles.
Ctrl: Control; TNF-α: Pre-stimulation of endothelial cells with TNF-α.

### Staining

Staining was performed at room temperature in a dark environment. After incubation with magnetic nanoparticles, HAECs were fixed with paraformaldehyde 3.75% for 20 min and washed three-times with phosphate-buffered saline (PBS) containing calcium and magnesium for 5 min.

The nucleus was stained with 4′6′ diamindine-2′phenylindole dihydrochloride (DAPI) 1 µM (Roche, Basel, Switzerland) for 10 min, washed twice with PBS, followed by cell permeabilization with Triton 0.1% for 5 min and cytoplasm labeling with 0.33 µM Phalloïdin Alexa Fluor®-568 (A34055, Invitrogen) in PBS for 30 min. Before the slides were filled with Dako fluorescence mounting medium (S302380), they were washed again twice with PBS.

### Confocal microscopy & image processing

Images were acquired with a confocal laser scanning microscope (CLSM; SP5; Leica, Heerbrugg, Switzerland), with a 63× N.A.1.4 oil immersion objective in the resonant mode. The following lasers were used to detect the labeling: 405-nm diode laser for the DAPI-stained nuclei, 488-nm argon laser 20% in the reflection mode for agglomerates of nanoparticles and 561-nm DPSS laser for the Phalloïdin Alexa Fluor®-568-stained cytoplasm.

Each experiment was performed three times. Four image series per slide were analyzed along *z*-stacks (0.13 µm z-step). Images were deconvolved (Huygens software, SVI, The Netherlands) and processed with the Imaris (Bitplane, Switzerland).

Agglomerates of magnetic nanoparticles were quantified with the Imaris 'spot function,' each spot measuring 0.601 µm$^3$. The spots representing agglomerates of particles located within the cells were separated from the agglomerates outside of the cells based on the actin (cytoplasm) channel. All spots representing agglomerated particles that showed a representative mean intensity for the cytoplasm channel were considered as being inside the cell (white spots), whereas agglomerates below this level intensity as outside of the cytoplasma (green spots).

### Assessment of inflammatory response of HAECs in the static model

#### ELISA

Supernatant was collected to determine the levels of human MCP-1 using an enzyme-linked immunosorbent assay ELISA (human MCP-1 ELISA Set BD OptEIA™ 555179, BD BIOSCIENCES, Allschwil, with a lower detection range of 1.0 pg/ml), and CINC-1 (recombinant human CXCL1/GROα/KC/CINC-1 ELISA kit, DY275, R&D Systems, Abington, UK, lower detection range 31 pg/ml).

### Assessment of viability of HAECs in the static model

#### LDH assay

Cytotoxicity was assessed using a colorimetric standard LDH assay (LDH CytoTox 96® Non-Radioactive Cytotoxicity Assay, Promega, WI, USA), measuring a stable cytosolic enzyme released during cell lysis according to the protocol of the manufacturer as previously described [13].

#### MTT assay

Cell viability was evaluated by MTT assay (MTT Formazan, Sigma Aldrich, Product number M2003), an *in vitro* method, based on the reduction of the yellow tetrazolium salt 3-(4,5-dimethylthiazol-2-yl)-2,5-diphenyltetrazolium bromide (MTT) to insoluble purple formazan crystals by living cells via mitochondrial dehydrogenates. A protocol was used as previously reported [13,14]. Because dehydrogenases are only active in living cells, conversion of MTT is therefore directly related to cell viability.

### Statistical analysis

R (R Core Team, 2014) with the lme4 package [15] were used to perform linear mixed effects analyses assessing the influences of different treatment modalities on particle uptake, cytotoxicity and inflammatory mediator expression in endothelial cells. With regard to the amount of particle uptake and diameter of agglomerates in endothelial cells, four randomly selected areas (28 × 32 µm$^2$) of each experimental approach (n = 3) were analyzed. Nanoparticle diameter was estimated according to: $\text{diameter}_{mNP}$ = (3 × volume/[4 × π]) ^ (1/3) × 2. As fixed effects, we entered shear stress, time of exposure and prestimulation with TNF (without interaction term) into the models. The four randomly selected areas were introduced in the mixed effect analysis as a random intercept nested with the experimental approaches. The respective experimental approach was introduced in the regression models using a random intercept. After visual inspection of residual plots, a log-transformation of the dependent

variable was performed if necessary. Parameter-specific p-values were obtained as described previously by Barr and colleagues [16]. Density plots were calculated using the 'ggplot2' package [17]. A p-value of <0.05 was considered statistically significant.

## Results

Poly(ethylene glycol)-functionalized ferromagnetic iron-carbide nanoparticles with a primary particle diameter of 30 nm and a magnetic saturation magnetization 123 emu/g were used for the experiments [8]. In order to compare various experimental conditions, a closed-loop circulation system was assembled (Figure 1). A flow cell lined with HAECs was connected to a tank containing the nanoparticles in cell culture medium. The nanoparticle dispersion was continuously sonicated to reduce aggregation of the ferromagnetic nanoparticles due to magnetic dipole–dipole interactions. Integrity of the cell layer lining the flow chamber was verified by CLSM for all experimental conditions. Fully adherent cells presenting intact actin filaments were found after the experiments indicating that shear stress (up to 3.22 dyn/cm$^2$) was well tolerated by HAECs for at least 30 min (Figure 2).

Endothelial nanoparticle uptake was investigated under conditions of different shear stress, exposure time and endothelial activation state by recording images with a confocal microscope at defined time points. In order to determine the uptake of particles into HAECs as well as the size of the agglomerates, CLSM images were semiquantitatively analyzed with Imaris (spot tracking of intra and extracellular particles). We found that with increasing shear stress (0, 0.57 and 3.22 dyn/cm$^2$) agglomerate uptake significantly decreased ($p < 0.001$; Figure 3A & Table 1). As expected, the higher the shear stress, the smaller was the mean diameter of the intracellular agglomerates ($p = 0.010$; Figure 3B & Table 2).

The influence of exposure time (5 and 30 min) was evaluated. No significant difference between 5 and 30 min of exposure to nanoparticles was observed with regard to the amount of agglomerate uptake in endothelial cells ($p = 0.945$) (Figure 3C & Table 1). But, the mean diameter of intracellular agglomerates was significantly lower when cells were exposed to nanoparticles for 30 in comparison to 5 min ($p = 0.001$) (Figure 3D & Table 2).

Following prestimulation of endothelial cells with TNF-α (1 ng/ml for 4 h prior to the flow experiment), we observed an accentuated uptake of agglomerates ($p < 0.001$) (Figure 3E & Table 1) with the mean diameter of agglomerates in HAECs being lower ($p < 0.001$) (Figure 3F & Table 2). Altogether, pre-stimulation of HAECs lead to an increased uptake.

With the findings from the dynamic model we then established a static model with a longer incubation time of stimulated endothelial cells with magnetic nanoparticles, thereby mimicking a potential situation of precapillary or capillary stasis with a prolonged exposure of endothelial cells to magnetic nanoparticles. Inflammatory mediator secretion in response to particle exposure was measured (Figure 4). Prestimulation of endothelial cells with TNF-α provoked an increased secretion of MCP-1 by 29 ng/ml ($p < 0.001$) (Figure 4A) and of CINC-1 protein by 1.6 ng/ml ($p < 0.001$) (Figure 4B). When endothelial cells were then incubated with magnetic nanoparticles, secretion of MCP-1 was reduced by 31%, CINC-1 expression by 56%. In summary, the inflammatory response of prestimulated endothelial cells was significantly less pronounced when followed by incubation with magnetic nanoparticles (Tables 3 & 4). To exclude cytotoxicity, lactate dehydrogenase (LDH) release (LDH assay) as well as NADPH oxidase-related metabolic activity (MTT assay) of HAECs were determined. Exposure to nanoparticles (2 or 4 h) as well as endothelial activation had no influence on endothelial cells with regard to viability/toxicity (overall $p = 0.343$) or metabolic activity (overall $p = 0.569$).

## Discussion

Targeted drug therapy with nanoparticles has been identified as promising future cancer therapy [18,19].

**Table 1. Mixed effect model on the influence of different treatment modalities on uptake of agglomerates of nanoparticles in endothelial cells.**

| Treatment | Coefficient | 95% CI | p-value |
|---|---|---|---|
| Increased shear stress | -0.008 | -0.011 to -0.004 | $p < 0.001$ |
| Exposure time of 30 min | 0.011 | -0.253–0.273 | $p = 0.945$ |
| Stimulation with TNF-α | 1.326 | 1.064–1.588 | $p < 0.001$ |

We analyzed four randomly selected areas (28 × 32 μm$^2$) of each experimental approach (n = 3). Exposure to stationary conditions over a time period of 5 min without TNF-α treatment has been defined as the reference group in the regression model (n = 178). The respective experimental approach was addressed in the mixed effect model using a random intercept. Dependent variable: amount of intracellular agglomerates of particles.

**Table 2. Mixed effect model on the influence of different treatment modalities on the diameter of agglomerates of nanoparticles in endothelial cells.**

| Treatment | Coefficient | 95% CI | p-value |
|---|---|---|---|
| Increased shear stress | -0.001 | -0.002 to -0.001 | p = 0.010 |
| Exposure time of 30 min | -0.113 | -0.171 to -0.055 | p = 0.001 |
| Stimulation with TNF-α | -0.164 | -0.220 to -0.108 | p < 0.001 |

We analyzed four randomly selected areas (28 × 32 μm²) of each experimental approach (n = 3). The diameter of nanoparticle agglomerates was estimated by diameter$_{mNP}$ = (3 × volume / [4 × π]) ^ (1/3) × 2. Exposure to stationary conditions over a time period of 5 min without TNF-α treatment has been defined as the reference group in the mixed effect model (n = 3284). Dependent variable: mean agglomerate diameter in endothelial cells.

While a number of conceptual approaches of how to reach tumors have been developed, a paucity of these works has focused on interaction of nanoparticles with cells of the vascular compartment. Recently published studies have highlighted the importance of assessing nanoparticle uptake under physiologically relevant conditions in order to collect meaningful data with regard to successful translation of *in vitro* findings into *in vivo* applications [20]. However, it has traditionally been considered difficult to reliably expose cells and tissue to magnetic nanoparticles under relevant exposure conditions [21].

Here, we demonstrate that shear stress and the presence of an inflammatory state are crucial factors determining the uptake of carbon-coated iron nanoparticles into endothelial cells in an *in vitro* model mimicking the venous vascular compartment. The higher the shear stress, the fewer intracellular agglomerates of particles were found intracellularly. Prolonged exposure time of up to 30 min did not favor agglomerate uptake, but intracellular agglomerates presented with a smaller mean diameter. Interestingly, a more pronounced particle uptake was observed in inflamed endothelial cells.

Successful guiding of magnetic nanoparticles loaded with chemotherapeutic agents to a tumor does not necessarily mean that less systemic reactions are evoked. While chemotherapy-induced adverse effects would likely be attenuated, the use of stable nanocarriers bears the risk of carrier-associated side effects, such as activation of the coagulation system or inflammation. In previous work we have carefully evaluated the effect of carbon-coated iron-carbide nanocarriers on blood coagulation components [22] and blood cells [5], and have not found any significant adverse effects. In this work, we substantially extended our knowledge on the interactions of carbon-coated iron-carbide

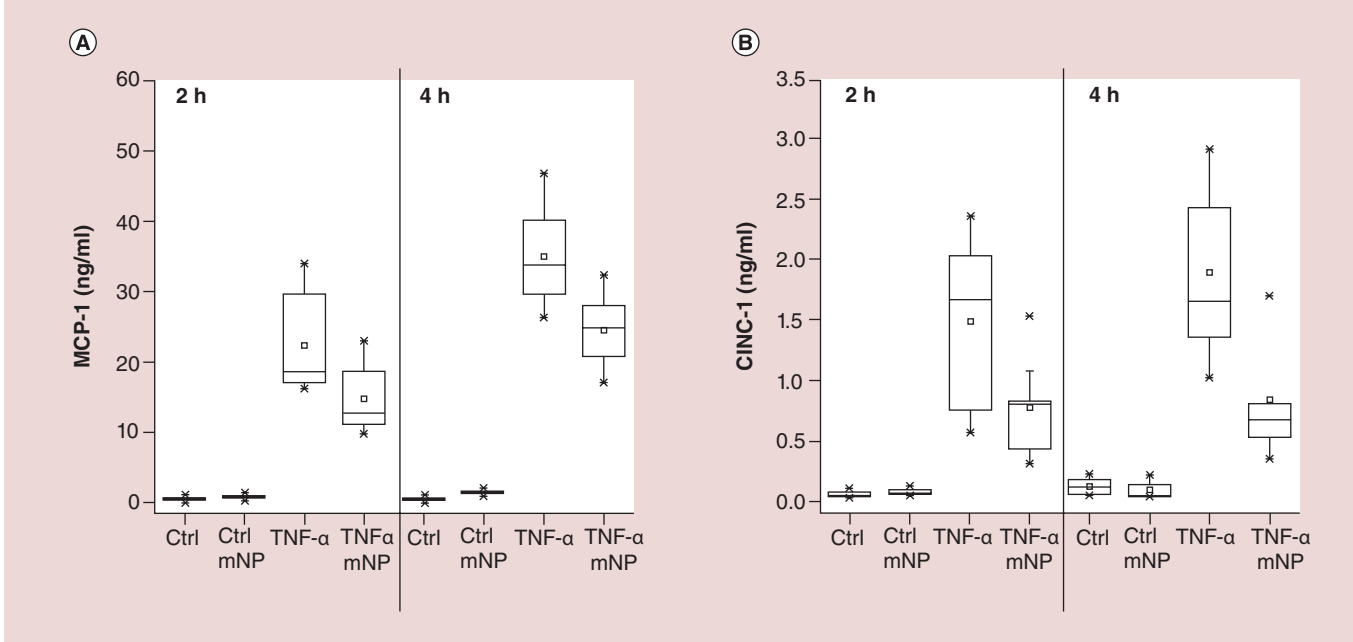


**Figure 4. Inflammatory response of endothelial cells after exposure to magnetic nanoparticles. (A)** MCP-1 expression after 2 and 4 h of exposure to magnetic nanoparticles. **(B)** CINC-1 expression after 2 and 4 h of exposure to magnetic nanoparticles.
Ctrl: Control; mNP: Magnetic nanoparticle; TNF-α: Pre-stimulation of endothelial cells with TNF-α.

Table 3. Mixed effect model on MCP-1 expression in response to nanoparticle exposure in noninflamed and inflamed endothelial cells.

| Treatment | Coefficient | 95% CI | p-value |
|---|---|---|---|
| Nanoparticle exposure | 1019 | -2763–4801 | 0.592 |
| Stimulation with TNF-α | 28,612 | 24,875–32,349 | <0.001 |
| Nanoparticle exposure + stimulation with TNF-α | 19,666 | 1582–23,507 | <0.001 |
| Exposure time | 3008 | 1689–4327 | <0.001 |

Exposure to stationary conditions over a time period of 5 min without TNF-α treatment has been defined as the reference group in the mixed effect model (n = 72). Dependent variable: MCP-1 (pg/ml).

nanoparticles with vascular compartment by studying the interactions of the nanoparticles with endothelial cells under standardized *in vitro* conditions [5].

The influence of shear stress, exposure time and endothelial activation on agglomerate uptake was investigated in a closed-loop flow system to allow a consistent comparison of experimental conditions (i.e., flow geometry, flow rates, exposure time and inflammatory state of cells) that otherwise is challenging to achieve under *in vivo* conditions. We found that increasing the shear stress lead to decreased nanoparticle uptake, corroborating results reported by Lin *et al.* for fluorescent carboxylated polystyrene nanoparticles [23]. Similarly, Samuel *et al.* have shown decreased uptake of 50-nm silica particles under conditions of shear stresses typically observed in postcapillary venules and peripherial arteries (shear stresses between 0.5 and 5 dyn/cm$^2$) [24]. In our study, there was no difference in overall particle uptake between 5 and 30 min exposure; however, difference might be detectable only after longer exposure times. A prolonged exposure to shear stress was not considered due to the possible impairment and detachment of the endothelial cell as previously demonstrated [24]. Finally, we found that uptake of magnetic nanoparticles was significantly enhanced upon preactivation of endothelial cells, which has potentially important consequences for both therapy (beneficial) and accidental exposure scenarios (harmful). The number of agglomerates in inflamed endothelial cells was strongly increased in comparison to control cells with the mean agglomerates size being smaller. These observations likely can be explained by an increased inflammation-induced permeability of the endothelial cells. Interestingly, we could see enhanced particle uptake of nanoparticles in inflamed endothelial cells even in absence of a targeting moiety (such as anti-ICAM-1 antibodies), as opposed to findings reported by Klingberg and colleagues for gold nanoparticles [25]. A possible interpretation would be that particles preferentially accumulate at inflamed sites. This could be due to increased vascular permeability similar to the enhanced permeability and retention effect observed in tumor tissue, and therefore might bring therapeutic benefits in inflammatory conditions. On the other hand, the limited uptake of magnetic nanoparticles in healthy endothelial cells under shear stress indicates that magnetic drug targeting may indeed be feasible as nonspecific uptake appears to be limited.

In order to further investigate the influence of particle exposure on the inflammatory response, we measured the cytokine release of HAECs in response to particle exposure under static conditions. We evaluated the inflammatory response by quantifying the release of two characteristic inflammatory mediators, MCP-1 and CINC-1 [26]. Following incubation of nanoparticles with unstimulated HAECs no inflammatory response was observed, indicating that particle exposure does not trigger an inflammatory response. In

Table 4. Mixed effect model on CINC-1 expression in response to nanoparticle exposure in noninflamed and inflamed endothelial cells.

| Treatment | Coefficient | 95% CI | p-value |
|---|---|---|---|
| Nanoparticle exposure | -6 | -282–269 | 0.964 |
| Stimulation with TNF-α | 1602 | 1326–1877 | <0.001 |
| Nanoparticle exposure + stimulation with TNF-α | 709 | 433–985 | <0.001 |
| Exposure time | 71 | -26–169 | <0.001 |

Exposure to stationary conditions over a time period of 5 min without TNF-α treatment has been defined as the reference group in the mixed effect model (n = 72). Dependent variable: CINC-1 (pg/ml).

TNF-α-prestimulated endothelial cells, however, a significant attenuation of the inflammation represented by a decreased expression of inflammatory mediators was found in response to magnetic nanoparticle exposure. This is an unexpected finding, which suggests an anti-inflammatory effect of the accumulated agglomerates of nanoparticles in endothelial cells, affecting the intracellular TNF-α signaling pathway, thereby attenuating the inflammatory response.

Importantly, the shear stress spectra investigated in the present *in vitro* flow cell model are also relevant for the intralymphatic application of nanoparticles as shear stresses in the lymph typically are in the order of 0.6 dyn/cm$^2$ [27]. Intralymphatic nanoparticle application has shown promising results in both tumor imaging and chemotherapeutics and a more detailed understanding of particle uptake in the lymphatic system using standardized *in vitro* models may pave the way for a rapid and safe development of more advanced imaging and theranostic probes [28].

## Conclusion

The present article highlights the importance of a thorough evaluation of potentially relevant exposure scenarios within the vascular compartment with regard to a future therapeutic administration of nanomaterials. Both shear stress and endothelial activation have pivotal effects on particle uptake and may significantly alter biodistribution under *in vivo* conditions.

## Future perspective

So far numerous *in vitro* as well as *in vivo* studies have been performed with nanomagnets providing promising results with regard to future cancer treatment using magnetic field guided drug targeting. Most of these studies have focused solely on therapeutic options, and consequently only few data exist regarding potential risks. The present data emerging from risk analysis further support feasibility of magnetic particle-based drug targeting and constitute an important cornerstone in the development of more sophisticated *in vivo* approaches as well as first-in-man trials.

### Author contributions

M Jacobson, BR Z'graggen, CM Schumacher, WJ Stark, IK Herrmann and B Beck-Schimmer designed research. M Jacobson, BR Z'graggen, CM Schumacher, C Dumrese, JM Mateos, C Aemisegger, U Ziegler and IK Herrmann did the experimental research. SMG and MU performed the statistical analysis. M Jacobson, BR Z'graggen, SM Graber, CM Schumacher, WJ Stark, M Urner, IK Herrmann and B Beck-Schimmer wrote the manuscript.

### Financial & competing interests disclosure

The authors kindly acknowledge the Swiss National Science Foundation, Berne, Switzerland, National Research Programme NRP64' Opportunities and risks of nanomaterials', Grant No. 406440-131268 (PI: B Beck-Schimmer, CO-PI: WJ Stark). WJ Stark declares ownership of shares of the company Turbobeads GmbH, a manufacturer of magnetic particles. The authors have no other relevant affiliations or financial involvement with any organization or entity with a financial interest in or financial conflict with the subject matter or materials discussed in the manuscript apart from those disclosed.

No writing assistance was utilized in the production of this manuscript.

### Executive summary

- Shear stress has major influence on nanoparticle uptake in endothelial cells.
- Inflammation of endothelial cells clearly increases endothelial nanoparticle uptake.
- A careful evaluation of the interactions of nanoparticles with the vascular system under dynamic conditions is of utmost importance with regard to successful translation of *in vitro* findings.

## References

1 Dobson J. Magnetic nanoparticles for drug delivery. *Drug Dev. Res.* 67(1), 55–60 (2006).

2 Arruebo M, Fernández-Pacheco R, Ibarra MR, Santamaría J. Magnetic nanoparticles for drug delivery. *Nano Today* 2(3), 22–32 (2007).

3 Sternberg N, Georgieva R, Duft K, Baumler H. Surface-modified loaded human red blood cells for targeting and delivery of drugs. *J. Microencapsul.* 29(1), 9–20 (2011).

4 Tavano R, Segat D, Reddi E *et al.* Procoagulant properties of bare and highly PEGylated vinyl-modified silica nanoparticles. *Nanomedicine (Lond.)* 5(6), 881–896 (2010).

5 Herrmann IK, Urner M, Hasler M *et al.* Iron core/shell nanoparticles as magnetic drug carriers: possible interactions with the vascular compartment. *Nanomedicine* 6(7), 1199–1213 (2011).

6 Herrmann IK, Grass RN, Stark WJ. High-strength metal nanomagnets for diagnostics and medicine: carbon shells allow long-term stability and reliable linker chemistry. *Nanomedicine* 4(7), 787–798 (2009).

7 Schumacher CM, Herrmann IK, Bubenhofer SB *et al.* Quantitative recovery of magnetic nanoparticles from flowing blood: trace analysis and the role of magnetization. *Adv. Funct. Mater.* 23(39), 4888–4896 (2013).

8 Herrmann IK, Grass RN, Mazunin D, Stark WJ. Synthesis and covalent surface functionalization of nonoxidic iron

core–shell nanomagnets. *Chem. Mater.* 21(14), 3275–3281 (2009).

9 Herrmann IK, Schlegel A, Graf R *et al.* Nanomagnet-based removal of lead and digoxin from living rats. *Nanoscale* 5(18), 8718–8723 (2013).

10 Herrmann IK, Urner M, Graf S *et al.* Endotoxin removal by magnetic separation-based blood purification. *Adv. Healthc. Mater.* 2(6), 829–835 (2013).

11 Mcbain SC, Yiu HH, Dobson J. Magnetic nanoparticles for gene and drug delivery. *Int. J. Nanomed.* 3(2), 169–180 (2008).

12 Han J, Zern BJ, Shuvaev VV, Davies PF, Muro S, Muzykantov V. Acute and chronic shear stress differently regulate endothelial internalization of nanocarriers targeted to platelet-endothelial cell adhesion molecule-1. *ACS Nano* 6(10), 8824–8836 (2012).

13 Wittlinger M, Schlapfer M, De Conno E *et al.* The effect of hydroxyethyl starches (HES 130/0.42 and HES 200/0.5) on activated renal tubular epithelial cells. *Anesth. Analg.* 110(2), 531–540 (2010).

14 Gray BP, Mcguire MJ, Brown KC. A liposomal drug platform overrides peptide ligand targeting to a cancer biomarker, irrespective of ligand affinity or density. *PLoS ONE* 8(8), e72938 (2013).

15 Bates D, Maechler M, Bolker B *et al.* Package 'lme4'. R Foundation for Statistical Computing, Vienna (2014).

16 Barr DJ, Levy R, Scheepers C, Tily HJ. Random effects structure for confirmatory hypothesis testing: Keep it maximal. *J. Mem. Lang.* 68(3), doi:10.1016/j.jml.2012.11.001 (2013).

17 Wickham H. *ggplot2: Elegant Graphics For Data Analysis.* Springer Science & Business Media, Berlin, Germany (2009).

18 Muddineti OS, Ghosh B, Biswas S. Current trends in using polymer coated gold nanoparticles for cancer therapy. *Int. J. Pharm.* 484(1–2), 252–267 (2015).

19 Prabhu RH, Patravale VB, Joshi MD. Polymeric nanoparticles for targeted treatment in oncology: current insights. *Int. J. Nanomedicine* 10 1001–1018 (2015).

20 Weissleder R, Nahrendorf M, Pittet MJ. Imaging macrophages with nanoparticles. *Nat. Mater.* 13(2), 125–138 (2014).

21 Peer D, Karp JM, Hong S, Farokhzad OC, Margalit R, Langer R. Nanocarriers as an emerging platform for cancer therapy. *Nat. Nano* 2(12), 751–760 (2007).

22 Bircher L, Theusinger OM, Locher S *et al.* Characterization of carbon-coated magnetic nanoparticles using clinical blood coagulation assays: effect of PEG-functionalization and comparison to silica nanoparticles. *J. Mater. Chem. B* 2(24), 3753–3758 (2014).

23 Lin A, Sabnis A, Kona S *et al.* Shear-regulated uptake of nanoparticles by endothelial cells and development of endothelial-targeting nanoparticles. *J. Biomed. Mater. Res. A* 93(3), 833–842 (2010).

24 Samuel SP, Jain N, O'dowd F *et al.* Multifactorial determinants that govern nanoparticle uptake by human endothelial cells under flow. *Int. J. Nanomedicine* 7 2943 (2012).

25 Klingberg H, Loft S, Oddershede LB, Moller P. The influence of flow, shear stress and adhesion molecule targeting on gold nanoparticle uptake in human endothelial cells. *Nanoscale* 7(26), 11409–11419 (2015).

26 Yue T, Roth Z'graggen B, Blumenthal S *et al.* Postconditioning with a volatile anaesthetic in alveolar epithelial cells *in vitro*. *Eur. Respir. J.* 31(1), 118–125 (2008).

27 Zawieja DC. Contractile physiology of lymphatics. *Lymphat. Res. Biol.* 7(2), 87–96 (2009).

28 Sevick-Muraca EM, Kwon S, Rasmussen JC. Emerging lymphatic imaging technologies for mouse and man. *J. Clin. Invest.* 124(3), 905–914 (2014).